scientific reports

Check for updates

OPEN

Mineralogical characteristics and color genesis of black quartzite jade from Linwu, Hunan, China

Haoyu Lu[1], Miao Shi[1,2,3,4]✉, Qinyuan Cao[1], Shiyu Ma[2], Xutong Zhao[2] & Xiangyu Wu[1]

The phanerocrystalline aggregate (single mineral particle size greater than 20 μm), which is mainly composed of α-quartz and has technological value, is called quartzite jade. Black quartzite jade from Linwu, Hunan Province, has gained significant market popularity due to its fine texture and aesthetic appeal. This study aims to provide a comprehensive analysis of this less-explored variety, focusing on its mineral composition, microstructure, spectral characteristics, and chemical properties. A combination of gemological assessments, polarizing microscopy, infrared spectroscopy, X-ray diffraction (XRD), total organic carbon (TOC) analysis, and X-ray fluorescence spectrometry (XRF) was utilized to investigate these features systematically. Additionally, the origin of color is discussed. Results indicate that the quartzite jade from Linwu primarily consists of α-quartz along with varying amounts of muscovite, andalusite, graphite, rutile, and other trace minerals. Infrared analysis reveals characteristic peaks at 479 cm^{-1}, 540 cm^{-1}, 778 cm^{-1}, 796 cm^{-1}, 1086 cm^{-1} and 1173 cm^{-1}. The presence of absorption double peaks between 700–800 cm^{-1} suggests enhanced particle arrangement within the internal structure of the sample; this indicates a well-organized Si–O bond configuration and a high degree of crystallization within the specimen. Based on metamorphic rock discriminant factor (DF) determinants showing negative values for all samples alongside an Al_2O_3 to TiO_2 ratio ranging from 19 to 29 implies these samples are medium to low-temperature metasomatic parametamorphic rocks formed via regional metamorphism, combined with the average total organic carbon (TOC) content of 1.27%, further suggesting that Linwu's quartzy autolith is silicon-rich clay shale. The predominant factor contributing to the sample's black coloration is attributed to its substantial graphite content.

Keywords Quartzite jade, Mineral composition, Geochemical characteristics, Color origin

Quartzite jade is a dense aggregate primarily composed of granular quartz, with individual mineral particle sizes generally exceeding 20 μm[1–3]. The metamorphically formed quartzite jade exhibits a compact structure resulting from the superposition of fine scales. From the crustal layer to the interior, the degree of crystallizationgradually diminishes, with most internal quartz existing in a cryptocrystalline form, making grain boundaries indistinguishable. In addition to quartz, the composition often includes sericite, muscovite, hematite, and andalusite[4,5]. The pure quartzite jade appears white. The green coloration in some specimens is attributed to ferrousiron in epidote, while others contain internal inclusions. Dongling jade and green dense jade derive their color from sericite lodged within quartz fractures[6]. The yellow and maroon varieties share a coloration mechanism with South Red Agate, primarily influenced by nano-micron-sized goethite and hematite within the interstitial spaces or fractures of quartz grains[7–9]. Nodular goethite imparts a yellow hue along the quartz particle interfaces, whereas red and black jade derive their color from hematite; thin hematite particles appear red, while thicker ones result in a darker, black coloration[10–12]. Tongtian jade, a high-quality quartzite jade newly identified in recent years in Hunan Province, comprises microcrystalline to cryptocrystalline quartz aggregates, occurring within iron-lithium mica-bearing granitic veins[13,14]. It belongs to a low-temperature hydrothermal replacement zone and is characterized by exquisite texture and vivid colors, making it highly valued for ornamental and collectible purposes[15]. Investigations into the geological background and mineralization patterns in the Xianghualing area of Hunan Province have revealed that Tongtian jade is predominantly colorless, with most specimens appearing pure white[16]. Its apparent coloration results from light refraction, emission, or absorption

[1]School of Earth Sciences, Hebei GEO University, Shijiazhuang 050031, China. [2]School of Gemology and Materials Science, Hebei GEO University, Shijiazhuang 050031, China. [3]Hebei Key Laboratory of Green Development of Rock Mineral Materials, Hebei GEO University, Shijiazhuang 050031, China. [4]Engineering Research Center for Silicate Solid Waste Resource Utilization of Hebei Province, Hebei GEO University, Shijiazhuang 050031, China. ✉email: miaoer727@126.com

through quartz crystal gaps. The clay minerals present within the jade can absorb trivalent iron ions or contain trace amounts of iron minerals such as pyrite, which oxidize to form red or yellow limonite; the greenish hues are due to unoxidized divalent iron ions in the mineral matrix[17]. Currently, research on black Tongtian jade remains limited. This study utilizes a range of analytical techniques, including gemological assessments, polarizing microscopy, infrared spectroscopy, X-ray powder diffraction (XRD), total organic carbon (TOC) analysis, and X-ray fluorescence (XRF) spectrometry, to investigate the spectral characteristics, mineral composition, microstructure, and chemical properties of black quartzite jade from Linwu, Hunan. The goal is to elucidate the origin of its coloration and establish diagnostic features specific to this unique jade variety.

Geological settings

The research area is located in the Xianghualing region, northern Linwu County, Hunan Province, near Tongtian Mountain, at an elevation of approximately 1600 m[15] (see Fig. 1). Geologically, it lies in the northern segment of the central Neoproterozoic–Early Paleozoic orogenic belt of South China, at the intersection of the Chenzhou–Linwu deep fault zone and anorth–south-trending fault system.The area has undergone three major tectonic stages: the geosynclinal stage, platform stage, and continental margin active belt stage[16]. The Caledonian orogeny formed an east–west-trending basement structure, later overprinted by a north–south-trending structural framework during the Indosinian orogeny. The Yanshanian orogeny further modified the region with northeast-trending faulted basins and large-scale faults, resulting in a triple tectonic superposition pattern. Magmatic activity peaked during the Yanshanian period, dominated by acidic granitic intrusions, which provided critical material sources for hydrothermal mineralization[18]. Quartzite jade primarily occurs within the Cambrian Tashan Group, hosted in fine-grained feldspathic quartz sandstone, Devonian micritic limestone, and clastic limestone interbedded with sandy shale. The ore body is structurally controlled, mainly distributed in the Tongtian Mountain and Xishan areas. The jade-bearing veins are closely associated with ferroleucite-bearing monzonitic granite, striking 62°–70°, extending 1 km, and dipping eastward. This distinct geological setting is highly favorable for quartzite jade mineralization and enrichment[17]. Quartzite jade is a trade or commercial term used to describe a fine-grained, compact, and often vividly coloured variety of quartzite that visually resembles jade. However, it's important to note that quartzite jade is not true jade in a mineralogical sense. True jade refers to two distinct minerals: jadeite and nephrite. In contrast, quartzite jade is composed primarily of microcrystalline or cryptocrystalline quartz (SiO_2), making it chemically and structurally very different[19]. Quartzite jade is typically derived from quartz-rich rocks such as sandstone that undergo regional or thermal metamorphism, which recrystallizes the quartz grains into a dense, hard rock. If colouring agents such as iron, manganese, or organic materials are present, they may impart a green or black hue that mimics jade[20–22].

Samples and methods

Sample

A total of 18 analysis and test samples of Tongtian Jade were collected and divided into three series of black, dark gray and light gray according to color (number: TJ-B-01 ~ 06, TJ-DG-01–06, TJ-LG-01 ~ 06, as shown in Fig. 2) from Tongtian area, Linwu , Hunan Province. The samples primarily exhibit a gray-black coloration, with a fine granular texture, earthy luster, and a glassy to waxy sheen; they are generally opaque. Some specimens also display surface features such as white needle-like inclusions, spotted minerals, white patches, yellow iron staining, and carbonate minerals. The refractive index of the samples ranges from approximately 1.53 to 1.54,

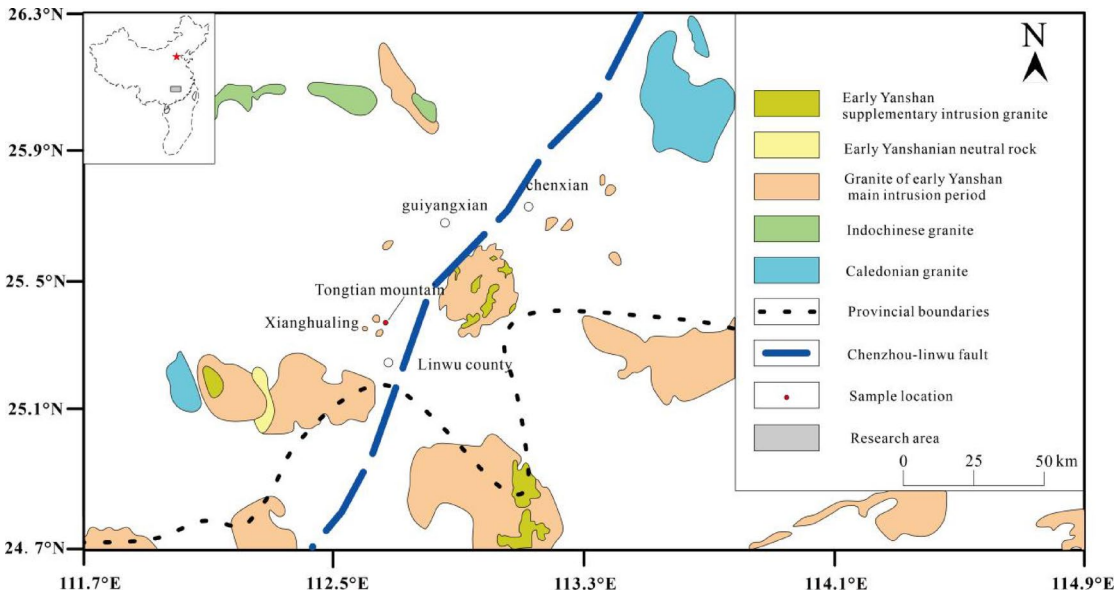

Fig. 1. Geological sketch of the study area (Be revised from Chen[23]).

Fig. 2. Photos of experimental samples.

with a density between 2.67 and 2.79 g/cm^3. The Mohs hardness was measured at 5.5, and the samples were found to be inert under both long- and short-wave ultraviolet light. The overall texture is notably fine-grained.

Polarized microscope

Thin sections (~0.003 cm) of the samples were prepared and analyzed using a Leica DW27009 polarized microscope at the Jewelry Testing Center, Hebei GEO University, to observe mineral composition.

Infrared spectroscopy (FTIR)

Fourier transform infrared (FTIR) spectroscopy was performed using a ThermoFisher IS 5 spectrometer at the Jewelry Testing Center, Hebei GEO University. The spectra were recorded in the 400–4000 cm^{-1} range with 32 scans at a resolution of 4 cm^{-1}.

X-ray diffraction (XRD)

XRD was performed using a Rigaku 9 kW diffractometer (Cu target, 45 kV, 200 mA) at 10° (2θ)/min over 3°–80°. Data were analyzed via Rietveld refinement in Jade 9 with the PDF2009 database.

X-ray fluorescence spectroscopy (XRF)

Elemental composition was analyzed using a SHIMADZU EDX-7000 XRF spectrometer (Rh target, 15 kV for Na–Sc, 50 kV for Al–U, 1000 μA, 5 mm collimator) under vacuum with the FP method.

Total organic carbon (TOC)

TOC content was determined following the Chinese standard GB/T 19145-2022 using a CS744 carbon–sulfur analyzer (LECO, USA) under an oxygen pressure of 0.25 MPa.

Results

Petrographic features

The primary mineral component of black quartzite jade in this region is quartz, with secondary minerals including andalusite (chiastolite), phlogopite, muscovite, and graphite. Trace amounts of rutile and ilmenite were also detected in certain areas. Polarizing microscope observations (Fig. 3) reveal that the sample exhibits a granular crystalline structure, with quartz grains characterized by jagged edges and granular morphology. These quartz grains display positive, low-relief features, with the highest interference colors reaching grade I yellow and white. The grain sizes range from 0.005 to 0.02 mm, predominantly between 0.01 and 0.015 mm, with indistinct grain boundaries and a relatively uniform distribution[24]. Andalusite (chiastolite) crystals are well-formed and heterogeneously distributed within the carbonaceous matrix, exhibiting a porphyroblastic texture. Additionally, numerous quartz fragments are interspersed within the carbonaceous and mica-rich matrix, forming a mottled texture. Significant amounts of carbon are aligned along the vertical bedding planes, presenting a fine granular structure. Abundant sheet-like and scaly graphite fills the intergranular spaces, displaying no light transmittance under single-polarized light. The matrix also contains granular and sheet-like quartz and mica, which are indicative of low-grade metamorphism typical of argillaceous rocks. The observed structural deformation of quartz, muscovite, and associated minerals reflects the effects of regional metamorphism on sedimentary rocks[25].

X-ray diffraction (XRD) analysis was performed using the K-value method to calculate and assess the semi-quantitative phase composition of the sample. The results revealed a diverse mineral assemblage, with spectral peaks corresponding to the superimposition of diffraction peaks from various mineral constituents. Detailed results are summarized in Table 1. The primary mineral identified in the samples was quartz, while secondary minerals included mica, feldspar, clay minerals, red stele, and trace amounts of rutile and ilmenite. The α-quartz content ranged from 24.6 to 32.6%, mica content varied from 18.9 to 23.6%, feldspar content was between 15.1 and 19.2%, and andalusite (chiastolite) ranged from 8.5 to 15.4%. The clay minerals were primarily chlorite and

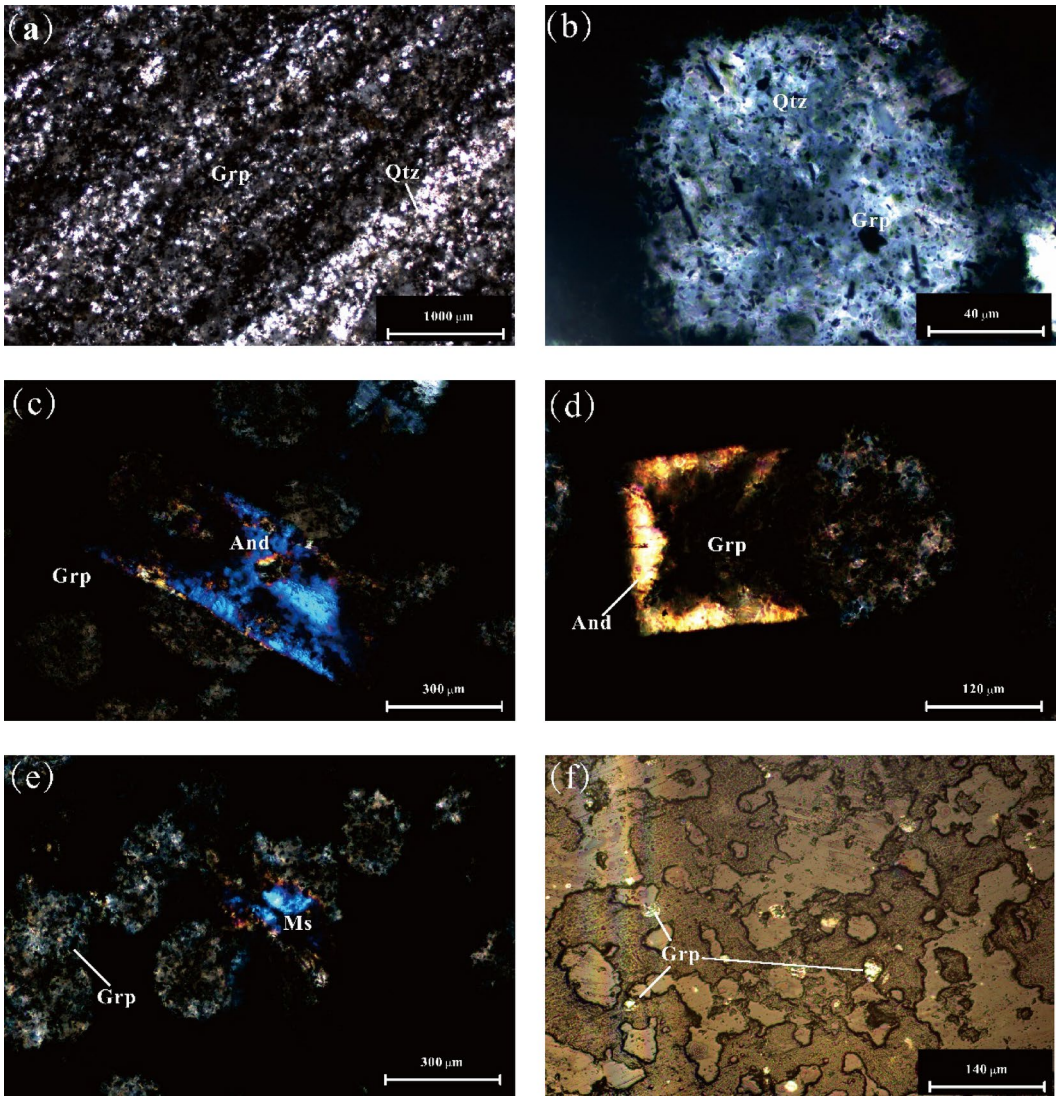

Fig. 3. Polariscope features of experimental samples. (**a**) Characteristics of stratified structures in sedimentary under single polarization. (**b**) Graphite: predominantly sheet-like and scaly, exhibiting light impermeability under single polarization; observed under 50 × single polarization. (**c**, **d**) Andalusite (Chiastolite): the cross-section appears rectangular with carbon inclusions; its cross-sectional shape resembles a hollow diagonal intersection at the center; interference colors transition from primary yellow to secondary violet; (**c**) is seen through 10 × orthogonal polarized light; (**d**) employs 20 × orthogonal polarized light. (**e**) Muscovite: heteromorphic flakes with faintly visible false hexagonal crystal forms; interference colors range from secondary blue to tertiary powdery hues;eis examined using 10 × orthogonal polarized light. (**f**) Graphite: under 20 × reflected light microscopy, the flake-like graphite exhibits a distinct metallic luster.

Number	α-Quartz	Mica	Feldspar	Andalusite	Rutile	Clay minerals	Titanium carbide	Ilmenite
TJ-LG-01	27.6	21.1	16.3	11.6	4.3	16.9	0.8	1.4
TJ-LG-04	29.1	20.3	16.3	10.8	4.8	16.6	0.9	1.2
TJ-B-01	25.2	21.6	15.7	10.5	5	19.6	0.9	1.5
TJ-B-02	26.6	23.6	15.1	9.9	4.4	18.1	0.7	1.6
TJ-B-03	25.4	18.9	16.1	15.4	4.7	17.1	0.9	1.5
TJ-DG-02	24.6	21.5	17.4	10.5	4.8	18.6	0.8	1.8
TJ-DG-04	32.6	19.2	19.2	8.5	3.7	14.9	0.6	1.3
Average	27.30	20.89	16.59	11.03	4.53	17.40	0.80	1.47

Table 1. Semi-quantitative analysis of mineral phases of experimental samples.

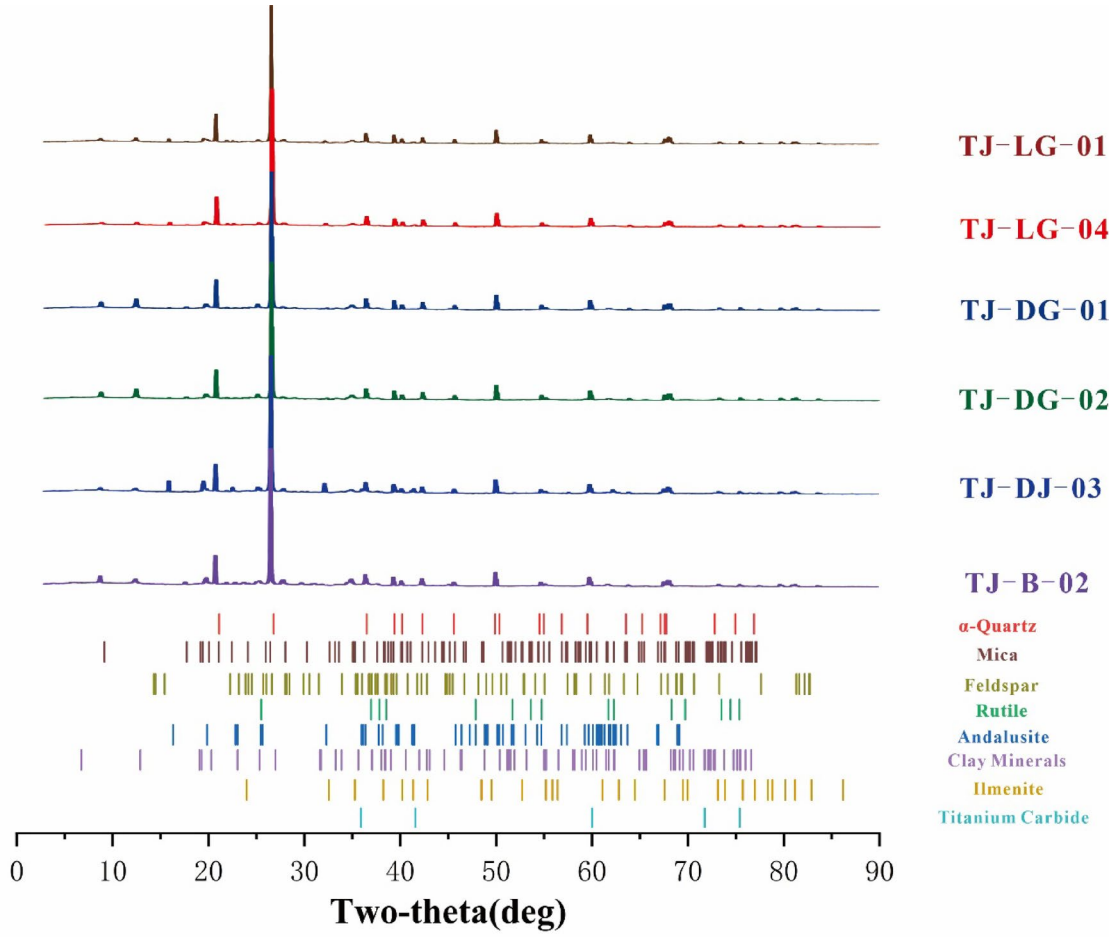

Fig. 4. X-ray diffraction graph of experimental samples.

Number	Lithology	TOC/%
TJ-LG-04	Quartzite	0.92
TJ-DG-02	Quartzite	1.04
TJ-B-04	Quartzite	1.72
TJ-B-06	Quartzite	1.40

Table 2. Total organic carbon (TOC) detection results of experimental samples.

kaolinite, with a content of 14.9–15.6%. Due to the small diffraction peak area, all clay minerals were quantified during the analysis. In most diffraction patterns, the peak spacings corresponded well with the PDF standard card for powder diffraction; however, some peaks exhibited slight deviations, which may be attributed to local structural effects during metamorphism. Based on the semi-quantitative analysis of the X-ray powder diffraction data and the microscopic observations, it can be preliminarily concluded that the black quartzite jade from the Linwu area in Hunan Province is a regional metamorphic rock. The specific diffraction peaks are shown in Fig. 4.

Total organic carbon (TOC) analysis was conducted on four samples. The results indicated that all samples contained organic matter. The average TOC content of Tongtian black quartzite jade from Linwu, Hunan Province was found to be 1.27%, with the specific data presented in Table 2.

Infrared spectroscopy features

The infrared spectrum of the sample (Fig. 5) shows a consistent pattern, with six prominent absorption peaks observed within the 400–1500 cm^{-1} range, specifically at 479 cm^{-1}, 540 cm^{-1}, 778 cm^{-1}, 796 cm^{-1}, 1086 cm^{-1}, and 1173 cm^{-1}. The bending vibrations observed between 300 and 600 cm^{-1} are attributed to Si–O, primarily around 479 cm^{-1} and 540 cm^{-1}, while the symmetrical stretching vibrations of Si–O–Si are located near 778 cm^{-1} and 796 cm^{-1}. The peaks at 1086 cm^{-1} and 1173 cm^{-1} correspond to Si–O vibrations[26]. These absorption bands align with the infrared spectrum characteristics of standard quartz. According to previous studies, the stretching vibrations of SiO_2 in quartz can reflect the degree of crystallization and the structural integrity of the sample[27].

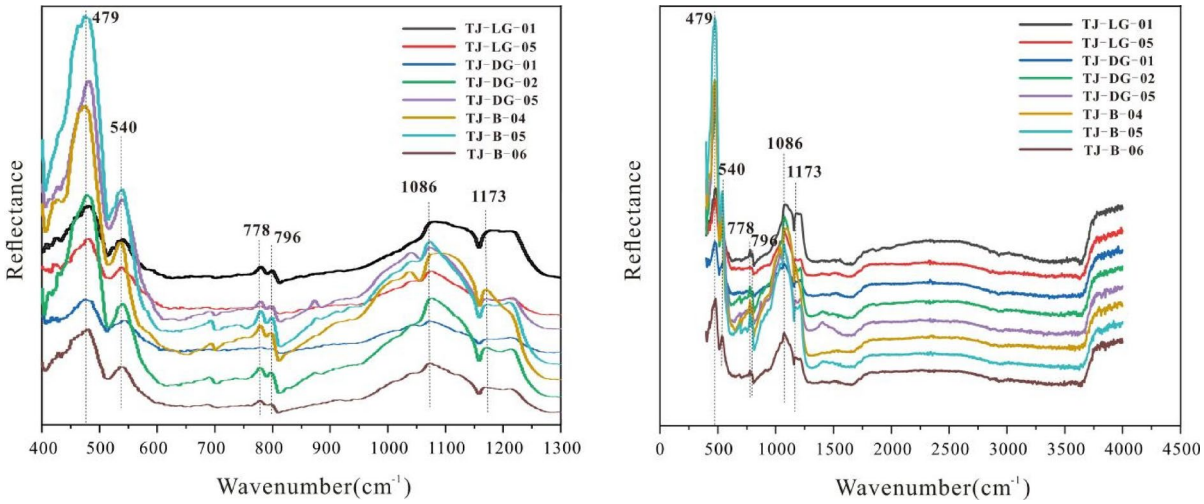

Fig. 5. Infrared absorption spectroscopy of experimental samples.

As quartz crystallinity improves, the absorption peaks between 700 and 800 cm^{-1} and 1000 and 1200 cm^{-1} transition from a single peak to a double peak, indicating the presence of shoulder absorption[28–30]. The observed double peaks at 778 cm^{-1} and 796 cm^{-1} suggest an enhancement in the internal structure of the sample, indicating well-ordered Si–O bonds and a high degree of crystallization[31,32].

Geochemical characteristics

Characteristics of the primary quantity elements

X-ray fluorescence spectroscopy of four samples averaged the percentage content in two decimal places. The main chemical composition of Tongtian black quartzite jade was SiO_2(63.87–74.69%), Al_2O_3 (13.90–20.49%), Fe_2O_3 (3.99–9.39%), K_2O (2.49–3.93%), and minor MgO (0.79–1.54%), CaO (0.41–2.63%), TiO_2 (0.50–1.07%), Na_2O (0–2.24%), MnO (0.06–0.16%), and Cr_2O_3 (0.01–0.03%). The average content is SiO_2(67.98%), Al_2O_3(18.36%), Fe_2O_3(6.35%), K_2O (3.12%), MgO (1.14%), CaO (1.00%), TiO_2(0.90%), Na_2O (0.56%), MnO (0.12%), and Cr_2O_3(0.02%).

Discussion

Genetic mechanism

Based on the analysis of X-ray fluorescence spectra, the SiO_2 content in the samples was consistently above 63.87%. According to the discriminant factor (DF) specification for metamorphic rocks, the original rock type of the sample can be determined using the formula:

$$DF = 10.44 - 0.21\ SiO_2 - 0.32\ Fe_2O_3 - 0.98\ MgO + 0.55\ CaO + 1.46\ Na_2O + 0.54\ K_2O.$$

Shaw, 1972, indicate that when DF > 0, the sample is classified as a positive metamaorphic rock, derived from an igneous protolith. Conversely, when DF < 0, the sample is a parametamorphic rock, originating from a sedimentary protolith[33]. The DF values calculated for each sample are as follows: – 5.18 (TJ-LG-03), – 5.60 (TJ-DG-01), – 3.46 (TJ-B-04 (1)), – 0.56 (TJ-B (2)), and – 2.06 (TJ-B-06). These results suggest that the DF values of the black quartzite jade samples in this region are all less than 0, thereby confirming that the samples from the study area are metamorphic rocks with a sedimentary protolith.

Girty and Ridge, 1996, demonstrated that the Al_2O_3/TiO_2 ratio serves as a key indicator for determining the characteristics of the protolith[34]. When this ratio is below 14, the protolith is likely to be derived from ferromagnetic deposits; when the ratio falls between 19 and 29, it may originate from felsic rock. The calculated Al_2O_3/TiO_2 ratios for the samples are as follows: 19.13 (TJ-LG-03), 20.46 (TJ-DG-01), 27.47 (TJ-B-04 (1)), 32.82 (TJ-B-04 (2)), and 19.24 (TJ-B-06). All the other three samples except TJ-B-04 are in the range of felsic rock sediments, the ratio of the Y-04 sample falls outside the range typically associated with felsic rock sediments, suggesting that the higher ratio observed in TJ-B-04 may be due to the presence of more andalusite (chiastolite). The samples are primarily composed of fine-grained quartz and feldspar, with a substantial amount of andalusite (chiastolite). Polarized microscope observations reveal a distinct stratified structure, indicating that the protolith is silicon-rich clay black shale.

According to previous studies, the Al_2O_3 / ($Al_2O_3 + Fe_2O_3$) ratio in sedimentary rocks can provide insights into the tectonic environment of rock formation. A value between 0.1 and 0.4 suggests a ridge environment; between 0.4 and 0.7 indicates a deep marine environment; and a value between 0.7 and 0.9 is characteristic of a continental environment[35,35]. The Al_2O_3 / ($Al_2O_3 + Fe_2O_3$) ratio for the study samples are 0.75(TJ-LG-03), 0.68(TJ-DG-01), 0.78(TJ-B-04 (1)), 0.79(TJ-B-04 (2)) and 0.77(TJ-B-06), which fall within the continental margin range, consistent with previous microscopic observations. Additionally, the regional metamorphic conditions for rock formation primarily involve an increase in temperature, leading to dehydration, recrystallization, and hydrothermal metasomatism of the protolith minerals. Polarized microscopy observations of the samples reveal granular and sheet-like quartz and mica, which conform to the characteristics of hydrothermal replacement

metamorphism. These findings support the conclusion that the mineralization process of the samples is due to hydrothermal replacement[37–39].

Color origin

Due to the Raman laser beam's size exceeding the particle diameter, obtaining a Raman spectrum of the sample was not feasible. However, based on previous research, the Tongtian black quartziteite jade from Linwu, Hunan province, primarily occurs within the Cambrian Tashan Group, comprising medium- to fine-grained feldspathic quartzite arenite, Devonian micrite, and clastic limestone interbedded with sandy shale[17]. During the Jurassic to Early Cretaceous, granitic magma intruded into the Cambrian strata. In the late stages of magma crystallization, hydrothermal differentiation produced highly acidic, silica-rich fluids, which rapidly cooled to form microcrystalline to cryptocrystalline quartzite aggregates[16]. TOC analysis suggests that organic matter within the protolith underwent burial and compaction during diagenesis, leading to alkane formation under reducing conditions. Subsequent thermal decomposition under specific temperature and pressure conditions generated elemental carbon, resulting in the presence of graphite in the metamorphic rock[40]. Microscopic observations confirm the uniform distribution of graphite throughout the sample and well developed stratified structure. Based on these findings, the protolith is inferred to be a silicon-rich, clay-rich black shale. The elevated graphite content in the quartziteite accounts for the black, opaque appearance of the originally transparent quartzite jade[41].

Conclusion

This study investigates the color origin of Tongtian black quartzite jade from Linwu, Hunan, through mineralogical, spectroscopic, and geochemical analyses. Results indicate that the primary mineral component is α-quartz (27.30%), with a granular crystalline texture characterized by quartz grains with zigzag edges (0.01–0.015 mm in diameter) and fuzzy grain boundaries. Secondary minerals include mica (20.89%), clay minerals (17.40%), feldspar (16.59%), and andalusite (chiastolite) (11.03%), along with minor rutile (4.53%), ilmenite (1.47%), and titanium carbide (0.80%). Infrared spectroscopy reveals characteristic absorption peaks at 300–600 cm^{-1}, 700–800 cm^{-1}, and 1000–1200 cm^{-1}, corresponding to the bending and stretching vibrations of Si–O bonds. The transition from unimodal to bimodal absorption peaks in the 700–800 cm^{-1} and 1000–1200 cm^{-1} ranges suggests increased internal structural order, with well-aligned Si–O bonds and a high degree of crystallinity. The chemical composition is dominated by SiO_2 (63.87–74.69%), with a total organic carbon (TOC) content of 1.27%. According to the discriminant factor (DF) criteria for metamorphic rocks, the samples are classified as parametamorphic rocks. Polarized microscopy reveals a distinct stratified structure, confirming that the protolith is silicon-rich clay black shale. The abundant graphite within the quartzite jade causes the originally transparent material to appear black and opaque.

Data availability

All data generated or analysed during this study are included in this published article.

Received: 22 November 2024; Accepted: 22 April 2025
Published online: 26 April 2025

References

1. Zhang, B, L. Systematic gemology 374–379 (Geological Publishing House, Beijing, 2006).
2. Li, S. R. Crystallography and mineralogy 188–190 (Geology Publishing House, Beijing, 2008).
3. Liu, X., Meng, Q., Chen, X. & Deng, S. Gemmological characteristics of quartzose jade by metamorphism. *J. Gems Gemmol.* **22**(1), 33–38 (2020).
4. Zhou, D, Y., Chen, H., Lu, T, J. & Ke, J. Comparative study on gemological characteristics of different colors of quartzy jade from Guilin, Guangxi. in *Proceedings of China International Jewelry Academic Exchange Conference*, 215–219 (2017).
5. Zhong, Q. et al. Compositions, structures and coloration mechanism of quartzite jade from Taxkorgan, Xinjiang. *J. Chin. Ceram. Soc.* **48**(1), 104–111 (2020).
6. Yu, J. G. Gemological and spectral characteristics of quartzite jade ("Dulong jade"). *J. Gems Gemmol.* **24**(03), 20–30 (2022).
7. Xiong, J, Z. Study on gem mineralogical characteristics of southern red agate in Liangshan Prefecture, Sichuan. (China Univ. Geosci., Beijing, 2015).
8. He, C. Understanding of several common quartzite jade. *West. Resour.* **4**, 33–34 (2017).
9. Cao, M. C. & Zhai, Y. M. Gemological properties and identification of southern red agate. *J. Changchun Inst. Technol.* **14**(03), 123–125 (2013).
10. Chen, Q. L. et al. Vibration spectral characterization of "she Taicui" jade. *J. Gems Gemmol.* **15**(2), 1–6 (2013).
11. Pan, Y. The study on gemological characteristics and genesis of Mixian County Jade from Henan (in Chinese, dissertation) (China Univ. Geosci., Beijing, 2017).
12. Bai, F. F. et al. Study on color mechanism of chicken blood jade from Guilin. *Miner. Petrol.* **36**(4), 1–9 (2016).
13. Jiang, W. T. Study on the geological characteristics and selectability of quartz sandstone in Yiliang County, Yunnan Province. *Chin. Non-Met. Miner. Ind.* **2**, 10–13 (2016).
14. Yang, X. H. Application research of DIMINE software in the prediction of jade mine resources in Tongtian. *Mining Technol.* **18**(4), 95–97 (2018).
15. Miao, X., Wang, L. S. & Shi, M. Mineralogical characteristics of the black quartzite jade in linwu district, Hunan province (Hebei GEO Univ., 2019).
16. Li, W. L. & Wang, Q. Preliminary exploration of the characteristics and the genesis of Tongtian Jade in Linwu County. *Land Resources Herald* **12**(4), 46–49 (2015).
17. Xu, Z. B., Zhang, L. J., Yang, X. H., Chen, H. L. & Yang, H. Y. Geological characteristics and metallogenic regularity of ore deposits of the black quartzite jade in Tongtian Mountain Linwu District, Hunan Province. *Resour. Inform. Eng.* **33**(5), 47–51 (2018).
18. Yuan, S. D. et al. Carbon, oxygen and strontium isotope geochemistry of calcites from the xianghualing tin-polymetallic deposit, Hunan Province. *Acta Geol. Sin.* **82**(11), 1522–1530 (2008).

19. Goswami, S., Bhagat, S., Maurya, V. K., Bhattacharjee, P. & Choudhury, D. K. A re-classification of Precambrian cherts: implication on diagenetic origin of chert concretion, nodule and geode. *J. Sediment. Environ.* **8**, 339–361 (2023).
20. Goswami, S., Mukherjee, A., Bhattacharjee, P. & Zakaulla, S. Primary sedimentary structures and MISS in Gulcheru quartzite along SW part of Cuddapah Basin. *J. Geol. Soc. India.* **89**(5), 511–520 (2017).
21. Goswami, S., Mukherjee, A., Zakaulla, S. & Rai, A. Microbial mat related features in Palaeoproterozoic Gulcheru formation and their role in low grade uranium mineralisation. *Int. J. Petrochem. Sci. Eng.* **1**(4), 83–89 (2016).
22. Goswami, S., Upadhyay, P. K., Saravanan, B., Natarajan, V. & Verma, M. B. Two types of uranium mineralization in Gulcheru quartzite: Fracture-controlled in Ambakapalle area, and litho-controlled in Tummalapalle area Cuddapah Basin, Andhra Pradesh, India. *Chin. Geol.* **2**, 142–156 (2019).
23. Chen, J., Wang, R. C., Zhu, J. C., Lu, J. J. & Ma, D. S. Tungsten-tin mineralization of granite in the Nanling multi-era. *Chin. Sci. Earth Sci.* **44**(1), 111–121 (2014).
24. Chang, L. H., Chen, M. Y. & Jin, W. A manual for thin section identification of transparent minerals 20–151 (Geological Publishing House, Beijing, 2006).
25. Chen, M. Y., Jin, W. & Zheng, C. Q. Handbook of metamorphic rock identification 41–73 Geological Publishing House, Beijing, 2009).
26. Luo, B., Yu, Y. F. & Liao, J. Spectral library and analysis for nondestructive testing of jewelry and jade 216–217 (China Univ. Geosci. (Wuhan), 2019).
27. Liu, D. R. Study on the spectroscopic characteristics of Dandong Yellow Chrismatite. *China gems & Jades.* **162**, 32–39 (2020).
28. Etchepare, J. Vibrational normal modes of SiO_2. I. α and β quartz. *J. Chem. Phys.* **60**(5), 1873–1876 (1974).
29. David, J. Quartzite development in early Palaeozoic nearshore marine environments. *Sedimentology* **60**(4), 1036–1058 (2013).
30. Li, J. J. et al. Infrared spectral features of SiO_2 with different crystallinity and their implications. *Infrared* **31**(12), 31–35 (2013).
31. Sylvester, P. Post-collisional strongly peraluminous granites. *Lithos* **45**(1), 29–44 (1998).
32. Etchepare, J., Merian, M. & Smetankine, L. Vibrational normal modes of SiO_2. I. α and β quartz. *J. Chem. Phys.* **60**(5), 1873–1876 (1974).
33. Shaw, D. M. The origin ofthe Apsley gneiss Ontario. *Can. J. Earth Sci.* **9**(1), 18–35 (1972).
34. Girty, G. H., Ridge, D. L., Knaack, C., Johnson, D. & Al-Riyami, R. K. Provenance and depositional setting of Paleozoic chert and argillite, Sierra Nevada, California. *J. Sediment. Res.* **66**(1), 107–118 (1996).
35. Zhou, W., Zeng, M., Wang, J., Zhang, L. & Li, Y. C. Determination of major elements and rare earth elements in rare earth ores by X-ray fluorescence spectrometry. *Rock Miner. Anal.* **37**(3), 298–305 (2018).
36. Jewell, P. W. & Stallard, R. F. Geochemistry and paleoceano graphic setting of central Nevada bedded barites. *J. Geol.* **99**(2), 151–170 (1991).
37. Hu, L., Liu, J. L. & Ji, M. *Handbook of deformation microstructure identification* 23–31 (Geological Publishing House, Beijing, 2015).
38. Klein, C. & Beukes, N. J. Geochemistry and sedimentology of a facies transition from limestone to iron-formation deposition in the Early Proterozoic Transvaal Supergroup, South Africa. *Econ. Geol.* **84**(7), 1733–1774 (1989).
39. Liu, S. X., Zeng, J. J., Zhang, X. K. & Qi, J. H. Superimposed metamorphism of the Gaolan Group in the eastern segment of Qilian orogenic belt. *Gansu Geol.* **29**(3), 22–28 (2020).
40. Lai, C, J. Geological characteristics and genesis of Huashan graphite deposit in Yihuang, Jiangxi Province. (Nanjing Univ., 2018).
41. Wang, H., Zhang, H. L. & Tan, J. M. Preliminary study of the effect of "dead carbon" on ^{14}C datin. *Carsol. Sin.* **23**(4), 299–303 (2004).

Acknowledgements

This work was supported by Funds for National Natural Science Foundation of China (Grant No.42002156), Natural Science Foundation of Hebei Province of China (Grant No.D2021403015), Excellent youth project of Hebei GEO University (Grant No.YQ202404), Hebei GEO University Student research project Funding (Grant No. KY202406).

Author contributions

H.L.: Conceptualization, Methodology, Formal analysis, Writing-original draft; M.S.: Conceptualization, Methodology, Funding acquisition, Writing—review & editing; Q.C.: Investigation; S.M.: Resources; X.Z.: Visualization; X.W.: Data curation.All author reviewed the manuscript and approved to publish.

Declarations

Competing interests

The authors declare no competing interests.

Additional information

Correspondence and requests for materials should be addressed to M.S.

Reprints and permissions information is available at www.nature.com/reprints.

Publisher's note Springer Nature remains neutral with regard to jurisdictional claims in published maps and institutional affiliations.